Macrocycle Anion Receptor

Anion Recognition by Partial Cone Dihomooxacalix[4]arene-Based Receptors Bearing Urea Groups: Remarkable Affinity for Benzoate Ion

Ana S. Augusto,[a] Alexandre S. Miranda,[a] José R. Ascenso,[b] Margarida Q. Miranda,[c] Vítor Félix,[c] Giovanna Brancatelli,[d] Neal Hickey,[d] Silvano Geremia,[d] and Paula M. Marcos*[a,e]

Abstract: Tetraureido-dihomooxacalix[4]arenes (*tert*-butyl **4a** and phenyl **4b**) were synthesised and obtained in a partial cone conformation in solution and in the solid state, as confirmed by NMR and X-ray diffraction studies. Their complexation ability towards halides, pseudo-halides and oxoanions was assessed by ^{1}H NMR and UV/Vis titrations. Structural and energetic insights of phenylurea **4b** complexes were also obtained using molecular dynamics (MD) simulations. The binding data showed that the association constants are strongly dependent on the nature of the substituent (alkyl/aryl) at the urea unit. *tert*-Butyl urea **4a** is a much weaker receptor than phenylurea **4b**, and showed association constants that decrease with decreasing of anion basicity. Phenylurea **4b** is a highly efficient anion receptor, exhibiting a remarkable binding ability towards BzO^- ion (log K_{ass} = 4.81). In comparison to the phenylurea analogue bearing a butyl spacer and a cone conformation, receptor **4b** containing a shorter spacer (three carbon atoms) and a partial cone conformation is more pre-organized, displaying a strong enhancement of its binding efficiency. MD simulations have shown that the anions are preferentially bound to the urea moieties of the macrocycle lower rim, in agreement with the ROESY spectrum carried out with phenylurea **4b** and BzO^- anion.

Introduction

Over the last ten, fifteen years, the complexation of anions has become a very important field of supramolecular chemistry. Applications involving anion recognition in different areas, such as sensing, extraction and separation, transport across membranes, organocatalysis and formation of supramolecular assemblies, have been particularly developed, as anions are present in many biological and environmental fields.[1,2] Amongst the halides, fluoride is important in dental health, but high levels of this ion in drinking water (> 1.5–2 mg/L) can cause fluorosis and water pollution, when discarded into rivers and seas.[3] Chloride and iodide are involved in many biological processes, such as transmembrane transport, and neurological activity and thyroid function, respectively, and the pseudo-halide cyanide is toxic even in trace amounts.[1,2] The carboxylates have various functions and uses, and nitrate and phosphates are harmful pollutants. The last-mentioned anion plays also a fundamental role in living systems.[1,2] Thus, the design and development of synthetic receptors that can selectively bind anions is still an area of growing importance.

Calixarenes,[4,5] and in particular the lower rim derivatives, are among those receptors,[6–8] as they represent a very versatile family of macrocycles in host–guest and supramolecular chemistry. The introduction of urea and thiourea units in the calixarene platform leads to receptors able to recognise anions by hydrogen-bonding interactions. These groups form strong and directional hydrogen bonds, producing highly preorganized receptors. Calix[4]arene-based anion receptors bearing (thio)urea groups are the most cited in the literature,[9–15] although ureidocalix[5]arene,[16] calix[6]arene[17–19] and thiacalix[4]arene[20] have also been reported.

Following our previous studies on anion binding by ureido dihomooxacalix[4]arenes[21–23] (calix[4]arene analogues in which one CH_2 bridge is replaced by one CH_2OCH_2 group),[24] we were interested in determining how the size of the spacer connecting the urea moieties to the calixarene skeleton (and consequently its conformation), as well as the number of hydrogen-bond donor sites would influence their binding affinity. In this context, recently, we reported the synthesis and the

[a] *Centro de Química Estrutural, Faculdade de Ciências da Universidade de Lisboa, Edifício C8, 1749-016 Lisboa, Portugal*
E-mail: pmmarcos@fc.ul.pt
https://cqe.tecnico.ulisboa.pt
[b] *Centro de Química Estrutural, Instituto Superior Técnico, Complexo I, Av. Rovisco Pais, 1049-001 Lisboa, Portugal*
[c] *Department of Chemistry, CICECO - Aveiro Institute of Materials University of Aveiro, 3810-193 Aveiro, Portugal*
[d] *Centre of Excellence in Biocrystallography, Department of Chemical and Pharmaceutical Sciences, University of Trieste, Via L. Giorgieri 1, 34127 Trieste, Italy*
[e] *Faculdade de Farmácia da Universidade de Lisboa, Av. Prof. Gama Pinto,*

anion complexation properties of three dihomooxacalix[4]-arenes in the cone conformation and containing four (thio)urea groups at the lower rim via a four carbon atom spacer.[23] This study showed that tetraphenyl urea is the strongest anion receptor. In comparison to related bidentate derivatives previously reported,[21,22] it is more preorganized and the higher number of potential hydrogen-bond donor sites provides a remarkable enhancement on its binding affinity, mainly to CN^- and Cl^- anions (log K_{ass} = 4.02 and 3.50, respectively). The selectivity is, in this case, controlled not only by the anion basicity, but also by its size.

In this paper we report the synthesis of two new inherently chiral *p-tert*-butyldihomooxacalix[4]arene tetra-substituted derivatives with *tert*-butyl or phenylurea moieties at the lower rim via a propyl spacer. Conformational analysis performed in solution by NMR and in the solid state by X-ray diffraction indicated the partial cone-1 conformation[25] for both receptors. Their complexation properties toward a variety of anions were assessed by proton NMR and UV/Vis absorption spectrophotometric titrations. Structural and energetic findings were rationalised with resort to MD simulations.

Results and Discussion

Synthesis, NMR and X-ray Characterisation of Tetraureas

Recently, we described the synthesis of three tetra (thio)ureido dihomooxacalix[4]arene derivatives in the cone conformation.[23] The (thio)urea residues, on the lower rim, were linked to the calixarene scaffold by a butyl spacer. With the aim of finding out how a shorter spacer would influence the anion complexation, we prepared two tetraureido dihomooxa receptors containing a three carbon atom spacer (Scheme 1). Thus, reaction of *p-tert*-butyldihomooxacalix[4]arene (**1**) with *N*-(3-bromopropyl) phthalimide and K_2CO_3 in refluxing acetonitrile afforded tetraphthalimide **2**, after purification by flash chromatography. Then, the phthalimido groups were removed with hydrazine in ethanol to give the tetraamine **3**, which reacted immediately with *tert*-butyl- or phenylisocyanate in chloroform to give the corresponding tetraurea derivatives (*tert*-butylurea **4a** and phenylurea **4b**). The conformation of these compounds in solution ($CDCl_3$ at room temp.) was investigated by NMR spectroscopy.

Compound **2** exhibits symmetric NMR spectra. The proton spectrum (Figure 1a) displays two singlets for the *tert*-butyl groups, three AB quartets (in a 2:2:1 ratio) for the CH_2 bridge protons and two pairs of doublets for the aromatic protons of the calixarene skeleton, besides several multiplets for the phthalimido groups and for the $–OCH_2CH_2CH_2N–$ methylene protons. The carbon-13 spectrum shows two $ArCH_2Ar$ resonances at δ = 30.7 ppm (two carbon atoms) and at δ = 30.2 ppm (one carbon atom), indicating the cone conformation.[26] In contrast with **2**, a complete absence of symmetry was observed in the NMR spectra of compounds **3**, **4a** and **4b** (Figure 1b–d), these receptors being inherently chiral. In the case of tetraureas, their ^1H spectra show four singlets for the *tert*-butyl protons, five AB quartets (or four and a pseudo-singlet) for the CH_2 bridge protons, four pairs of doublets for the aromatic protons, and four triplets and four singlets for the NHa and NHb protons, respectively. In addition, the methylene protons of the propyl spacers display several multiplets, with some of them experiencing upfield shifts (as for example –0.25 and 0.07 ppm for the $–OCH_2C\boldsymbol{H}_2CH_2N–$ protons of phenylurea **4b**). This reveals a

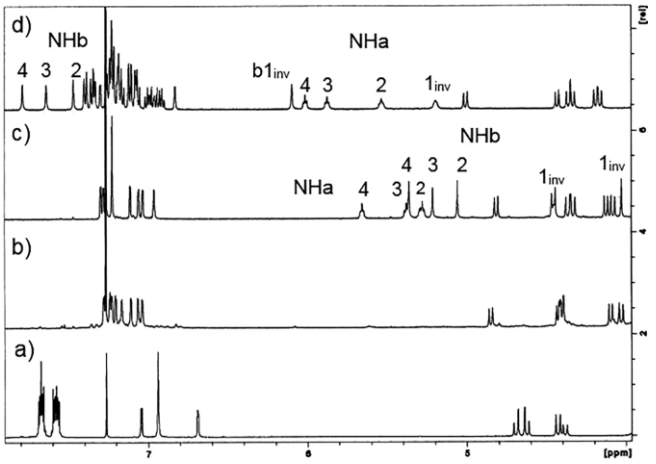

Figure 1. Partial ^1H NMR spectra (500 MHz, $CDCl_3$, 25 °C) of (a) phthalimide **2**, (b) amine **3**, (c) *t*Bu-urea **4a**, (d) Ph-urea **4b**.

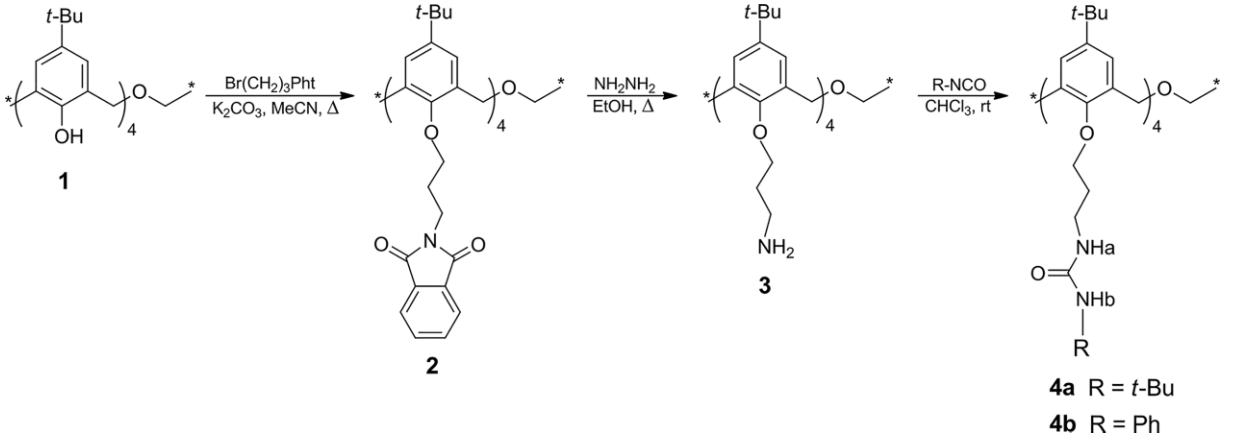

Scheme 1. Synthetic route for the preparation of tetra-urea derivatives **4a** and **4b**.

shielding effect for those CH_2 protons due to the aromatic rings, and consequently that the phenol residue containing that substituent group is inverted. The ^{13}C NMR spectra exhibit three $ArCH_2Ar$ resonances, two around 30 ppm and one at 37 ppm, indicating the partial cone-1 conformation (Scheme 2).[25] The proton assignments were confirmed through 2D NMR spectra (COSY, NOESY and ROESY experiments).

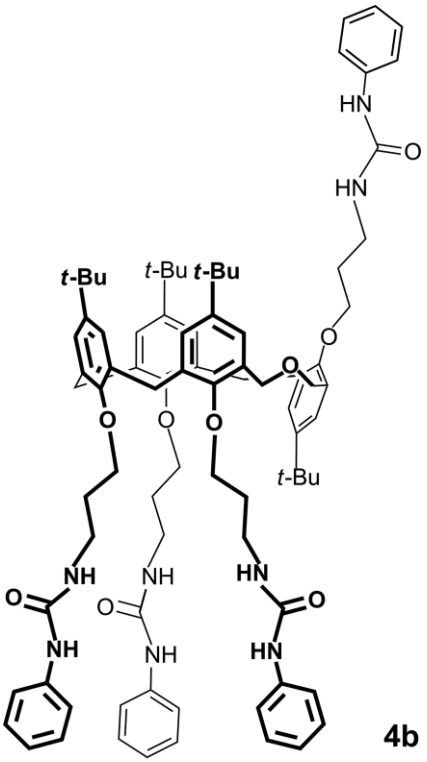

Scheme 2. Phenylurea **4b** in the partial cone-1 conformation.

Single crystals suitable for an X-ray investigation were obtained by slow evaporation of solutions containing compounds **4a** and **4b**. In the case of compound **4a** two different crystalline forms were obtained (hereafter denominated **4aα** and **4aβ**), using a 1,4-dioxane/ethanol mixture and ethanol as solvents, respectively. Crystals of compound **4b** were obtained from a solution with a $CHCl_3$/DMSO mixture as solvent. The structure determinations reveal that the asymmetric units of all three monoclinic cells contain one dihomooxacalix[4]arene molecule. All macrocycles show partial cone conformations (Figure 2), with one aryl ring (A) projecting downwards from the mean plane defined by the bridging oxygen and carbon atoms. The partial cone conformation, in conjunction with the CH_2OCH_2 bridging, generates an interesting inherent chirality in the dihomooxacalix[4]arene structures[27] compared to partial cone calix[4]arenes, for which inherent chirality can be attained only with a minimum of two different substituents. Dihomooxacalix[4]arenes with four equivalent upper rim and four equivalent lower rim substituents exhibit a total of 10 different conformational isomers including four enantiomeric couples (Figure 3). A method to assign a descriptor (M/P)[28] for the absolute configuration in these systems is proposed in Figure 3.

All three crystal structures have been solved in centrosymmetric space groups, therefore the compound is present as a racemic mixture for all three. For one of the structures (**4aβ**) an almost complete overlap of two enantiomers (M and P) has been observed in the asymmetric unit. The resulting disorder is chiefly found on the aromatic ring containing the outward ureido group, which occupies two apparent positions in order to accommodate the CH_2OCH_2 bridge on different sides of the ring. The two crystalline forms **4aα** and **4aβ** show comparable conformations of the dihomooxacalix[4]arene cavities, as summarised in Table 1. In both cases the opposing B and D rings show large outward angles with respect to the dihomooxa-

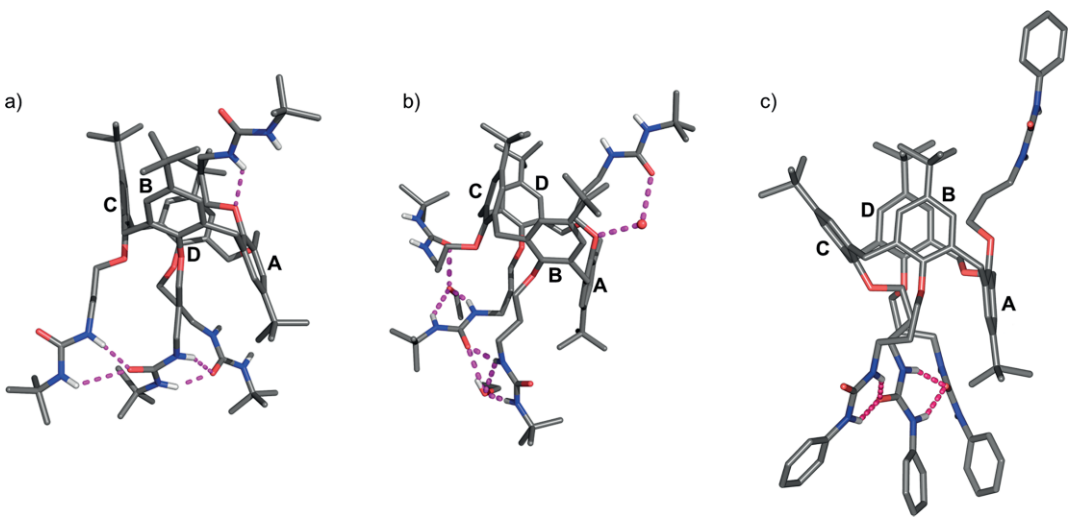

Figure 2. Solid state structures of compounds **4aα**, **4aβ** and **4b**. The asymmetric unit contains one macrocycle together with one and a half 1,4-dioxane solvent molecules for **4aα** (a), one macrocycle together with one half water molecule and one and a half ethanol solvent molecules for **4aβ** (b), and one macrocycle together with a DSMO molecule with partial occupancy for **4b** (c). The labels of the four aryl rings that define the macrocycle cavity are also shown. Solvent molecules, all hydrogen atoms and selected disordered non-hydrogen atoms and hydrogen atoms have been omitted for clarity. The ureido fragments at the lower and upper rim are involved in networks of double intra and intermolecular N–H···O hydrogen bonds (see text and Figure S1 for details). Intramolecular H-bonds are represented by dashed lines in magenta.

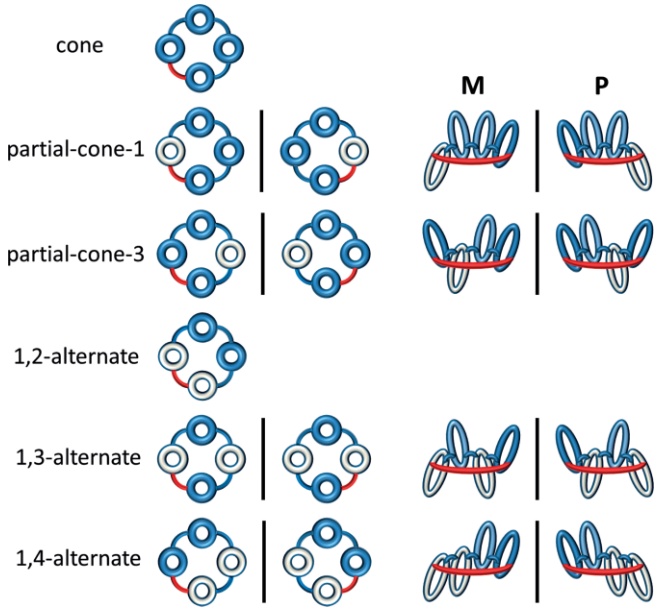

Figure 3. Schematic representation (top view) of the 10 conformational isomers of dihomooxacalix[4]arene. Mirror planes which relate the four enantiomeric couples are shown as vertical lines. The oxa bridge is represented in red and the different arene orientations are represented by different colours. The absolute configuration (M/P) of the four enantiomeric couples (side view, with the oxa bridge in foreground) are defined by the clockwise (P) and anticlockwise (M) rotation of the propeller formed by two oppositely oriented arenes connected by the oxa-bridge (excluding the partial cone-3 conformation for which the oppositely oriented arene couple in background must be considered as the propeller).

calix[4]arene mean plane, defined by the oxygen and carbon atoms of the bridging groups, ranging from 138° to 111°, whereas rings C are almost perpendicular to this plane. Rings A are inclined outwards from the underside of the mean plane, which result in acute inward supplementary angles with respect to the upper side. The propyl spacers partially occupy the calixarene cavities, however the phenomenon is less pronounced for **4aβ** due to differences in the hydrogen bonds formed by the two structures (vide infra).

Table 1. Dihedral angles between the aryl planes and the mean plane of the bridging methylene carbon atoms for compounds **4aα**, **4aβ** and **4b**.

	A	B	C	D
4aα	65.5(1)	137.8(1)	98.7(1)	111.3(1)
4aβ[a]	85.6(1)	113.8(1)	95.4(1)	137.1(1)
	69.4(3)	134.0(1)	95.8(1)	120.2(1)
4b	81.1(1)	93.4(1)	132.4(1)	85.4(1)

[a] For **4aβ**, the dihedral angles shown in the second row those made by the second component of the disorder (40 % occupancy).

The conformation of the cavities of the phenyl derivative (**4b**) shows significant differences with respect to the *tert*-butyl analogue structures (**4aα** and **4aβ**). In this case, rings B and D are almost perpendicular to the mean macrocycle plane (93° and 85°, respectively), while ring C shows the largest outwards deviation from the mean plane (132°). Ring A, orientated downwards, is almost perpendicular to the mean plane (inward dihedral angle of 81°) and its propyl spacer does not occupy the calixarene cavity.

The orientation of the oxygen atom of the CH_2OCH_2 bridge with respect to the calixarene partial cone shows an interesting variation across the three structures: for **4b** and **4aα** it is orientated towards the cavity and away from the cavity, respectively. The **4aβ** conformer with highest occupancy (60 %) exhibits an intermediate upward orientation, while the second component (40 %) shows a conformation similar to **4aα**.

As observed in Figure 2 and Figure S1, the ureido groups at the lower and upper rims of both macrocycle molecules are involved in analogous networks of intra- and intermolecular N–H···O double hydrogen bonds, albeit with significant differences in the overall packing arrangements. Details of the H-bond lengths are listed in Table S1. The crystal packing of **4aα** shows three of the four ureido groups involved in two intramolecular N–H···O double hydrogen bonds (Figure 2a). The H_2N_2C H-bond donor group at the terminal of these two intramolecular H-bonds forms a double intermolecular H-bond with the C=O H-bond acceptor group on the outwards ureido of a symmetrically equivalent molecule (Figure S1a). This results in chains of dihomooxacalixarene molecules generated by glide planes. In addition, the two NH donors on the outward ureido group form two distinct H-bonds: an intramolecular H-bond with the ether oxygen atom on the same chain as acceptor and a H-bond with one of the oxygen atoms on a 1,4 dioxane solvent molecule (Figure 2a and Figure S1a). The former results in the rather compact configuration of the chain involved, which partially occupies the calixarene cavity, while the latter interconnects the above-described chains of dihomooxacalixarene molecules in an antiparallel fashion (Figure S1a).

In the case of **4aβ**, a significantly different hydrogen bond network and packing arrangement is observed. With regard to the three iso-orientated ureido groups, the ethanol molecules disrupt the above-described pattern of two double intramolecular N–H···O double hydrogen bonds among the three groups (Figure 2b). Thus, in Figure 2b only one intramolecular hydrogen bond is maintained: a single intramolecular N–H···O hydrogen bond between one of the ureido H_2N_2C donor groups (involving the NH group nearest to the aromatic ring) and the carbonyl acceptor group of a second, middle ureido group. The second NH donor forms an intermolecular hydrogen bond with the oxygen atom of an ethanol molecule, which in turn forms an O–H···O hydrogen bond with the same carbonyl acceptor of the middle ureido group. Thus, the ethanol molecule is inserted into the intramolecular hydrogen bond network, similarly to the anion binding sites proposed by the MD studies (vide infra). The carbonyl acceptor oxygen of the first ureido is involved in N–H···O double hydrogen bonds with the outwards ureido group of a symmetrically related molecule, resulting in chains of dihomooxacalixarene/ethanol molecules generated by glide planes (Figure S1b). The third iso-oriented ureido group is more isolated from the other two as there is no intramolecular hydrogen bond with the other two. Instead, an ethanol molecule bridges between this and the middle ureido groups (Figure 2b). One of the NH donor groups of the middle ureido group (the NH nearest the aromatic ring) forms an N–H···O

hydrogen bond with the oxygen atom of the ethanol molecule, which forms an O–H···O hydrogen bond with the carbonyl oxygen acceptor of the third ureido group. Thus, in this case the ethanol solvent molecule completely disrupts the intramolecular hydrogen bond network observed in **4aα**. The H_2N_2C donor of this third ureido group forms a double intermolecular hydrogen bond with the carbonyl group on the outwards ureido group of an equivalent molecule in an adjacent cell, forming chains on equivalent molecules related by translation (Figure S1b). Finally, a disordered water molecule bridges the ether and carbonyl oxygen atoms along the chain of the outward ureido group (Figure 2b). It should be noted that, to allow the formation of this bridge, this outward chain is rotated with respect to the orientation observed in **4aα**. The comparison of **4aα** and **4aβ** shows that the ability of the solvent molecules to act as a hydrogen donor or acceptor, or both, strongly influences the hydrogen bond pattern observed.

In the case of **4b**, a rather different packing arrangement arises from a similar set of hydrogen bonds to that observed in **4aα**. In the same way as described above, three of the four ureido groups are also involved in intramolecular N–H···O double hydrogen bonds (Figure 2c). However, it should be noted that the double H-bonds observed in **4b** are more symmetrical compared to those observed in **4aα**, where one N–H···O bond length is significantly longer than the other (Table S1). Both ureido terminals (the H_2N_2C H-bond donor group, and the C=O H-bond acceptor group) of these intramolecular H-bond chains form further intermolecular N–H···O double hydrogen bonds with the outwards ureido group of two other dihomooxacalix[4]arene molecules. This produces an extended one dimensional H-bond network in which each outward ureido group is found between the other three ureido groups on different molecules, thereby forming a chain composed of alternating pairs of intra- and intermolecular H-bonds (Figure S1c).

Attempts to co-crystallise **4a** and **4b** in the presence of various salts containing the anions under investigation resulted in crystals of the calixarene without the anions.

Anion Binding Studies

The complexation properties of tetraureas **4a** and **4b** in the presence of a large variety of anions of different geometries (spherical: F^-, Cl^-, Br^-, I^-; linear: CN^-, SCN^-; trigonal planar: NO_3^-, AcO^-, BzO^- and tetrahedral: HSO_4^-, $H_2PO_4^-$, ClO_4^-) were studied in $CDCl_3$ by ^1H NMR titrations using tetrabutylammonium (TBA) salts. The association constants, as log K_{ass} reported in Table 2, were determined through the WinEQ NMR 2 program,[29] following the urea NH chemical shifts. In a few cases where these proton signals became broad or even disappeared, the association constants were calculated from the complexation induced shifts of the aromatic *ortho* protons of the phenyl group (**4b**) or of the $ArCH_2Ar$ axial protons of the calixarene skeleton.

The addition of TBA salts to the receptors resulted in downfield shifts of their NH protons (see for example **4b** + Cl^- in Figure S2), clearly indicating hydrogen bonding interactions between the urea groups and the anions. In all cases, only one set of signals was observed for the complexed and free host, showing a fast exchange rate on the NMR time scale at room temperature. The titration profiles obtained (Figure 4 and Figure 5) indicate the formation of 1:1 receptor-anion complexes, this stoichiometry being also confirmed by Job plots (Figure S3 and Figure S4). However, in the case of $H_2PO_4^-$ and Ph urea **4b**, the Job plot shows the curve maximum at 0.3 mol fraction of **4b**, indicating a 2:1 (anion:receptor) complex (Figure S5). This 2:1 stoichiometry had already been reported with a di-substituted partial cone ureido-calix[4]arene compound.[11] The data in Table 2 show that *t*Bu urea **4a** is a moderate receptor, exhibiting the strongest binding for F^- (log K_{ass} = 2.60). Toward the spherical halide and the linear pseudo-halide anions, the association constants decrease with decreasing of anion basicity. Concerning the oxoanions, either the trigonal planar or the tetrahedral geometries, a slight inversion of the basicity order was observed (AcO^-/BzO^- and $HSO_4^-/H_2PO_4^-$), being however within the experimental error. This was previously reported with other dihomooxa receptors.[21,23] The log K_{ass} values obtained for **4a** are almost identical to those obtained with the *t*Bu urea analogue bearing a butyl spacer and presenting a cone conformation.[23] This seems to indicate that a smaller number of potential hydrogen-bond donor sites (six instead of eight), together with the less flexible urea arms induced by a shorter spacer (only three carbon atoms), yield a receptor with similar anion affinity.

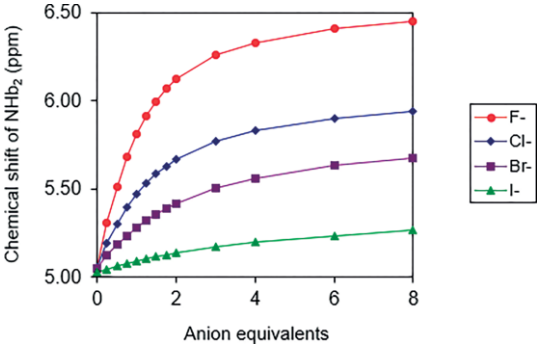

Figure 4. Titration curves of *t*Bu-urea **4a** with TBA salts in $CDCl_3$..

Table 2. Association constants (log K_{ass})[a] of dihomooxa tetra ureas **4a** and **4b** determined by **NMR** and UV/Vis in chloroform at 25 °C.

	Spherical				Linear		Trigonal Planar			Tetrahedral		
	F^-	Cl^-	Br^-	I^-	CN^-	SCN^-	NO_3^-	AcO^-	BzO^-	HSO_4^-	$H_2PO_4^-$	ClO_4^-
I. Radius [Å][b]	1.33	1.81	1.96	2.20	1.91	2.13	1.79	2.32	–	1.90	2.00	2.40
*t*Bu-urea **4a**	**2.60**	**2.40**	**2.10**	**1.78**	**2.16**	**1.75**	**2.16**	**2.29**	**2.39**	**1.95**	**1.86**	**1.82**
	3.50	3.18	2.95	–	–	–	2.93	3.27	3.40	3.25	3.18	–
Ph-urea **4b**	**4.19**	**4.55**	**3.66**	**2.83**	**4.20**	**3.01**	**3.38**	**4.21**	**4.81**	**3.96**	–[c]	**2.56**

[a] Estimated error < 10 %. [b] Data quoted in I. Marcus, *Ion Properties*, Marcel Dekker, New York, pp. 50–51, **1997**. [c] Undetermined stoichiometry.

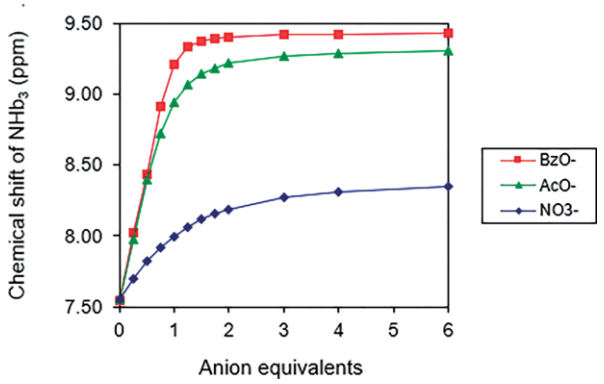

Figure 5. Titration curves of Ph-urea **4b** with TBA salts in $CDCl_3$.

Binding studies of *t*Bu urea **4a** with some anions of different geometries (F^-, Cl^-, Br^-, NO_3^-, AcO^-, BzO^-, HSO_4^- and $H_2PO_4^-$) as TBA salts were also performed by UV/Vis absorption spectrophotometry in $CHCl_3$. Significant changes were observed in the absorption spectra of **4a** upon the addition of the anions, as shown for example in Figure 6 for F^-. The association constants obtained (Table 2) follow the same trend of those determined by ^1H NMR studies, although on average they are one log unit higher. This can be explained by the different concentration range employed in both methods: 5×10^{-3} M for NMR and 5×10^{-5} M for UV/Vis absorption. The more diluted solutions (one hundred times) used in the UV titrations favour the dissociation of the salts, providing a higher concentration of the anions available for complexation, and resulting in higher association constants. Similar results were previously reported in the literature.[12,16,20]

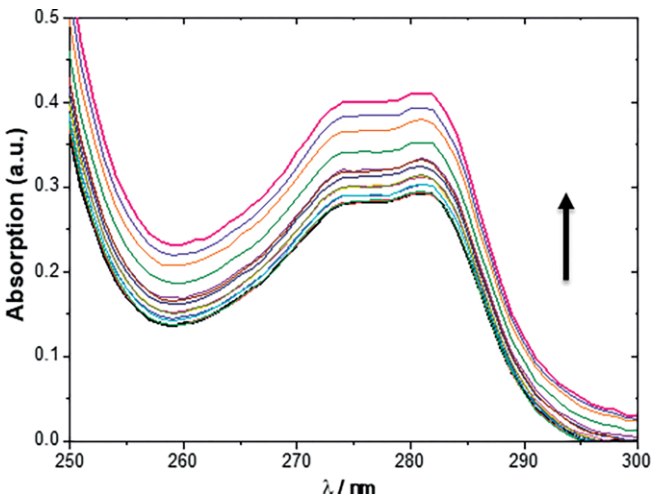

Figure 6. Changes in the UV spectra of *t*Bu-urea **4a** (5×10^{-5} M) upon addition of TBA *F* (up to 10 equiv.) in $CHCl_3$. The arrow indicates the increasing amounts of salt.

With regard to Ph urea **4b**, the ^1H NMR titrations were carried out at a slightly lower concentration (8.3×10^{-4} M) due to solubility problems. As shown by the data in Table 2, the substituents (aryl/alkyl) at the urea residue strongly influence the association constants. Ph urea **4b** is a very effective receptor, displaying from good to very good affinity toward all the anions. Among the spherical halides, **4b** shows a strong selectivity peak for Cl^- (log K_{ass} = 4.55), with some inversion of the anion basicity order. Fluoride and chloride induce large downfield shifts of the NH protons. For example, the addition of 2 equiv. of TBA F and TBA Cl caused a downfield shift for the urea NHb_2 proton of 2.33 and 1.18 ppm, respectively. The preference for Cl^- suggests that the anion size dominates over the anion basicity, as already observed with the tetraphenylurea analogue containing a four carbon atom spacer.[23] The insertion of a propyl spacer between the urea moieties and the calixarene scaffold renders **4b** in a less flexible and consequently more preorganized macrocycle in comparison with its Ph urea analogue bearing a butyl spacer (log K_{ass} = 3.50).[23] An enhancement of one order of magnitude is obtained for Cl^- complexation, suggesting a very suitable size complementarity between **4b** and the anion. In the presence of the pseudo-halides, the association constants decrease in order of the anion basicity, with CN^- showing a log K_{ass} = 4.20. Concerning the trigonal planar oxoanions, **4b** displayed a remarkable affinity for BzO^-, exhibiting the highest association constant ever found with a dihomooxa urea receptor. In this case, the log K_{ass} value is increased by almost two log units, from 2.93 for the butyl spacer analogue[23] to 4.81 for **4b**, and by 1.3 log units for the AcO^- anion (log K_{ass} = 2.89 and 4.21, respectively). Towards the carboxylates, there is also an inversion of the basicity order. This has been observed for the majority of the dihomooxa urea receptors studied so far, although the differences between the two anions are very small (Δlog $K_{ass} \leq 0.10$), within the experimental error. For **4b**, however, the Δlog K_{ass} BzO^-/AcO^- is 0.60, corresponding to a ratio of association constants of 4. In this case, the complexation of BzO^- by **4b** may benefit from π stacking interactions, combined with the cooperative effect of all hydrogen bonding. A similar preference for BzO^- anion was reported with di- and tri-substituted ureido-calix[4]arene compounds.[11] The tetrahedral oxoanion HSO_4^- was also tightly bound by this receptor (log K_{ass} = 3.96).

The association constants reported in Table 2 were obtained using the NH chemical shifts of the three urea arms (lower rim). When the constants were calculated using the NH chemical shifts from the inverted urea arm (upper rim) different situations were found. In the case of *t*Bu urea **4a**, presenting lower association constants (log $K_{ass} \leq 2.60$), the latter values were almost identical to the former. This does not indicate an effective binding by the inverted ureido moiety, rather it reflects the conformational changes undergone by the calixarene molecule upon complexation. For Ph urea **4b**, slight decreases in the log K_{ass} values were obtained for I^-, SCN^- and ClO_4^- (Δ = 0.16, 0.26 and 0.31, respectively), corresponding to the less bound anions. Towards the remaining anions, this difference substantially increases as the association constants increase, reaching a maximum for BzO^- (Δ = 2.60), followed by Cl^- and HSO_4^- (Δ = 1.53 and 1.47, respectively). In order to demonstrate that the anions are binding to the lower rim ureido groups, a ROESY spectrum was carried out with Ph urea **4b** + 3 equiv. of TBA BzO. Strong NOE correlations between the three NHb protons of the lower rim ureido groups and the aromatic *ortho* protons of the benzoate anion were observed, as shown in Figure 7, as

well as weak correlations between the NHa protons and the anion. No ROESY peaks were observed between NHa+b protons of the inverted arm and benzoate anion. These results indicate that the BzO^- anion is bound to the lower rim urea moieties.

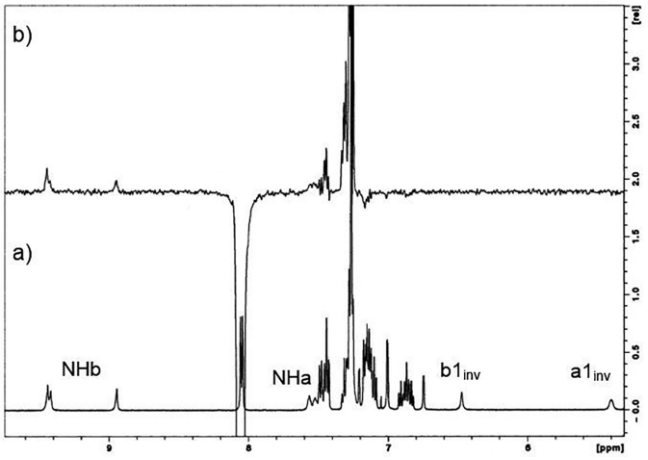

Figure 7. Ph-urea **4b** + 3 equiv. of TBA benzoate (500 MHz, $CDCl_3$, 25 °C). (a) Partial ^1H NMR spectrum, (b) cross section of the ROESY spectrum at the benzoate *ortho* protons (δ =8.05 ppm) showing correlations with the urea lower rim NH protons.

The calixarene skeletons of these partial cone urea compounds seem to undergo deeper conformational changes upon complexation when compared to those observed for the cone butyl spacer analogues,[23] since the *tert*-butyl and the aromatic protons significantly change their positions. Further analysis of the ROESY spectrum together with the observed trend in the displacements of the aromatic and *tert*-butyl peaks of the calixarene skeleton during the titration, allowed the assignment of the new *tert*-butyl and aromatic positions in the complex (Figure S6). Thus, a maximum chemical shift variation of 0.17 ppm was observed for one of the four *t*Bu groups, while the inverted one displayed a minimum variation of 0.05 ppm upon the addition of 3 equiv. of TBA BzO to **4b**. Concerning the aromatic protons, two of them experience large upfield shifts of 0.55 and 0.35 ppm, two others experience downfield shifts of 0.20 and 0.19 ppm, while the remaining display small variations (0.09–0.03 ppm).

Molecular Modelling

Structural insights into anion binding ability of the Ph urea **4b** for an extensive range of anions, including spherical halides, linear (CN^- and SCN^-), trigonal (NO_3^-, AcO^- and BzO^-) and tetrahedral anions (HSO_4^- and $H_2PO_4^-$) were further obtained through MD simulations in chloroform carried out with Amber 16.[30] **4b**, the anions and TBA counterion were described with force field parameters taken from GAFF[31,32] and RESP charges.[33] A discrete atomic charge of –1 was assigned to the halides, which were described with vdW parameters taken from reference[34]. The remaining computational details are given in the Supporting Information.

Two binding scenarios were investigated using the partial cone conformation obtained from the crystal structure of **4b**. In the first binding scenario (**A**), the anion was positioned in the lower rim of **4b**, surrounded by three convergent urea binding units, while in the second one (**B**), the anion was located in the upper rim, held by a single urea binding unit. Subsequently, these binding arrangements were submitted to MD runs in gas phase at 700 K and the lowest energy conformation obtained for each complex was then immersed in a cubic box of $CHCl_3$ all-atom model.[35] These systems were then simulated under periodic boundary conditions along two independent runs of 50 ns each.

Overall, each anion is kept hydrogen-bonded to **4b**'s lower rim urea binding units, maintaining the initial binding scenario **A** throughout the simulation time, as illustrated in Figure 8a with representative snapshots of the MD simulations with chloride, thiocyanate, benzoate and hydrogensulfate anions. Equivalent structural features were found for the other anions with the same binding geometry, as depicted in Figure S7. Moreover, the TBA counterion, initially positioned away from the solvated complex, quickly diffuses towards it, sealing the anion within the lower rim binding pocket. The counting of the hydrogen bonding interactions between the anion and the urea binding sites for scenario **A** is summarised in Table 3, together with their dimensions (see Table S2 for the complete statistics). The four halides are recognised by up to 6 hydrogen bonding interactions which are intermittently maintained with the largest anion having the lowest number of hydrogen bonds. The N•••X interaction distances (X = F^-, Cl^-, Br^- or I^-) mirror the halides' size (Table 3). The linear CN^- is lodged between the three urea binding units, mainly adopting a vertical disposition, perpendicular to the mean plane defined by the methylene bridges (vide supra), with either C or N atoms pointing to the calixarene ring, as illustrated in Figure S7d. This oscillation leads to an average of 4.53 ± 0.86 hydrogen bonds established between the urea binding units and the C atom of the anion and 4.91 ± 0.86 hydrogen bonds with the N atom. The longer SCN^- also rotates within the binding pocket, without a preferential spatial disposition (Figure 8b), leading to more intermittent hydrogen bonding interactions as indicated by the average numbers of N–H···S and N–H···N of 2.68 ± 1.16 and 2.90 ± 1.13, respectively. In the case of the trigonal anion NO_3^- associated with **4b** (Figure S7f), the hydrogen bonds are intermittent, with the oxygen atoms of the anion being swapped between the three urea convergent binding units. Furthermore, the average number of N–H···O_3N hydrogen bonds, 7.93 ± 1.07, indicates that the oxygen atoms are shared between neighbouring binding units. The more basic AcO^- and BzO^- anions are recognised by their carboxylate groups (Figure S7e and Figure S8c), which are also shared between the urea binding units, while the methyl and phenyl groups point away from the binding pocket, without any permanent synergetic interaction with the phenyl urea rings. On average, the N–H···O_2C interactions amount to 6.88 ± 0.48 and 6.91 ± 0.64 for AcO^- and BzO^-, respectively. The tetrahedral anions, HSO_4^- and $H_2PO_4^-$, present similar behaviours throughout the MD simulations, being encapsulated with the oxygen atoms establishing intermittent hydrogen bonding interactions with the three binding units, as illustrated in Figure 8d and Figure S7g, respectively. As expected, these inter-

molecular interactions are mainly established with the non-protonated oxygen atoms, yielding averages of 7.30 ± 1.12 and 7.09 ± 0.91, for HSO_4^- and $H_2PO_4^-$. On the other hand, MD simulations in binding scenario **B** show that the anionic guests are held by a single urea binding unit throughout the MD sampling time, while the three binding units on the lower rim are stabilised by intramolecular hydrogen bonds (Figure 9 and Figure S8, and Table S3 for the average dimensions of these intermolecular interactions). These structural results are unsurprising considering that $CHCl_3$ is a non-competitive media.

Table 3. Average dimensions[a] and counting of hydrogen bonding interactions[b] between **4b** and the guest anions in scenario **A**.

Anion	N···X [Å][c]	N–H···X [°][c]	Total hydrogen bonds
F^-	2.869 ± 0.120	158.4 ± 7.7	6.00 ± 0.00
Cl^-	3.383 ± 0.147	160.2 ± 8.7	5.98 ± 0.13
Br^-	3.571 ± 0.157	160.6 ± 8.8	5.91 ± 0.30
I^-	3.840 ± 0.175	159.5 ± 10.5	5.05 ± 0.93
CN^-	3.076 ± 0.155	160.5 ± 9.8	9.44 ± 1.00
SCN^-	3.179 ± 0.207	156.3 ± 10.9	5.58 ± 0.71
NO_3^-	2.954 ± 0.165	155.8 ± 11.5	7.93 ± 1.07
AcO^-	2.893 ± 0.142	157.3 ± 9.4	6.88 ± 0.48
BzO^-	2.934 ± 0.202	156.3 ± 10.4	6.91 ± 0.64
HSO_4^-	2.969 ± 0.194	153.6 ± 13.2	7.30 ± 1.12
$H_2PO_4^-$	2.910 ± 0.154	155.7 ± 10.7	7.09 ± 0.91

[a] N = 48000. [b] N = 8000. [c] X = O, N, S or halide.

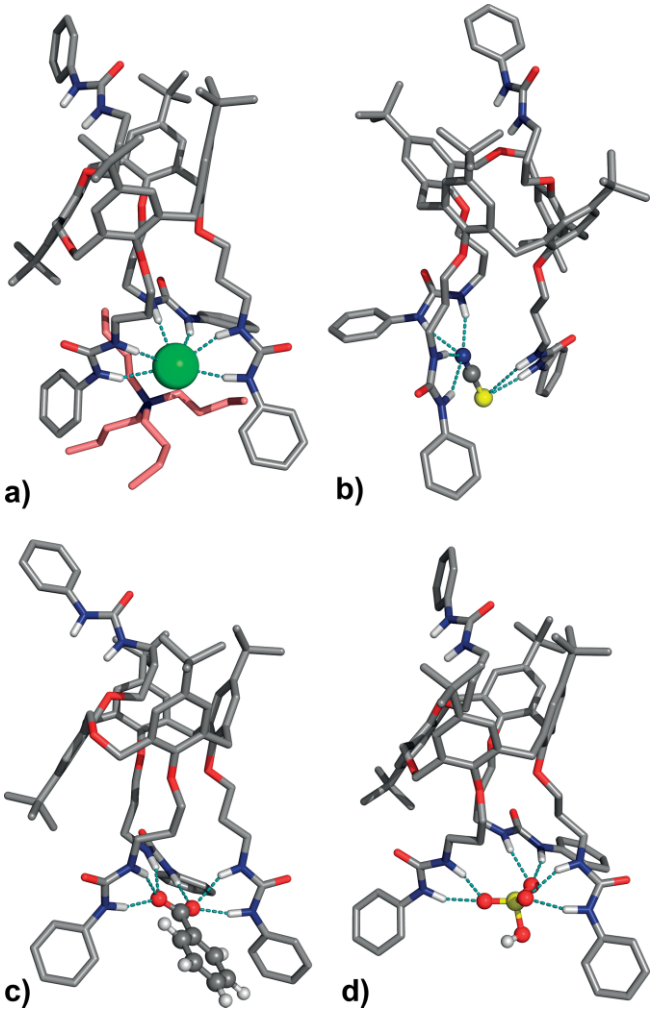

Figure 8. Illustrative snapshots of **4b** complexes with Cl^- (a), SCN^- (b), BzO^- (c) and HSO_4^- (d) in scenario **A**, with the anions being recognised by the three binding units via hydrogen bonds (light blue dashed lines). **4b** and TBA (in a) are drawn in sticks, while the anions are shown in spheres (halide) or in ball-and-sticks model (polyatomic anions), following the CPK colouring scheme. The solvent and TBA molecules (b–d), as well as the non-polar hydrogen atoms, were hidden for clarity.

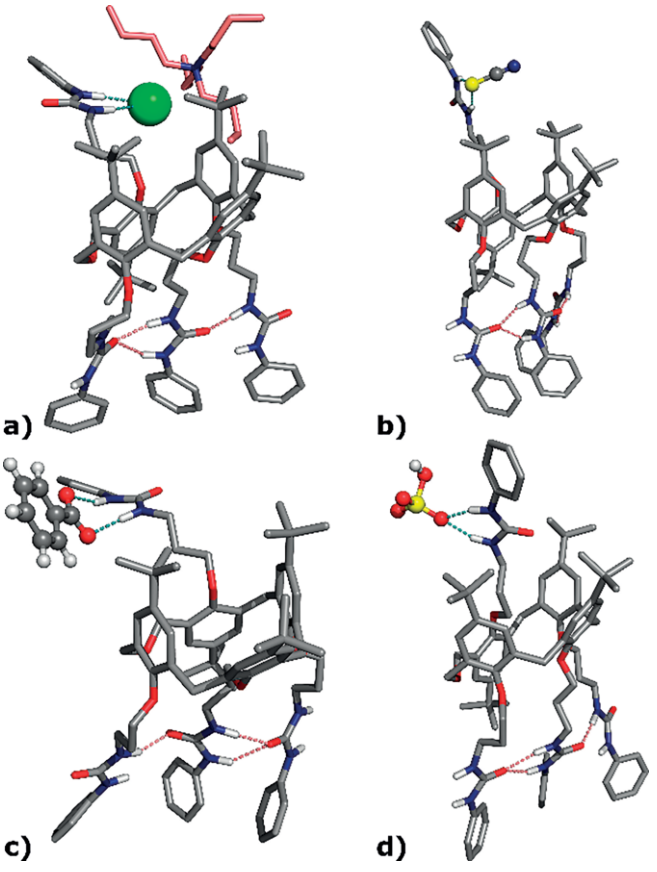

Figure 9. Illustrative snapshots of **4b** complexes with Cl^- (a), SCN^- (b), BzO^- (c) and HSO_4^- (d) in scenario **B**, with the anions being recognised by a single binding unit via hydrogen bonds (light blue dashed lines), while the three binding units on the lower rim are stabilised by intramolecular N–H···O=C hydrogen bonds (pink dashed lines). Remaining details as given in Figure 8.

In agreement with the Job plot for Ph urea **4b** and $H_2PO_4^-$ (Figure S5), the complex with a 1:2 stoichiometry was also investigated (Figure 10), placing the anion in each calixarene rim and bound to the urea units, as in scenarios **A** and **B**. Subsequently, this complex was simulated in two independent MD runs of 50 ns. Both phosphate anions are firmly held to the binding units via hydrogen bonding interactions. In addition, in the upper rim, the two concomitant hydrogen bonds between the single urea binding unit and the anion are kept throughout the simulation time, as indicated by an average total number of hydrogen bonds of 2.14 ± 0.37. In contrast, in the lower rim, these interactions are intermittently maintained with the anion swapping between the hydrogen binding sites of six urea units

leading to a total number of hydrogen bonds of 6.81 ± 0.96. In agreement, the average dimensions of the N–H···$H_2PO_4^-$ hydrogen bonds in the upper rim are shorter with lower standard deviations than those estimated for the lower rim (Table 4). These MD simulations show that the **4b**·$H_2PO_4^-$ 1:2 complex can occur in a non-competitive solvent, such as $CHCl_3$.

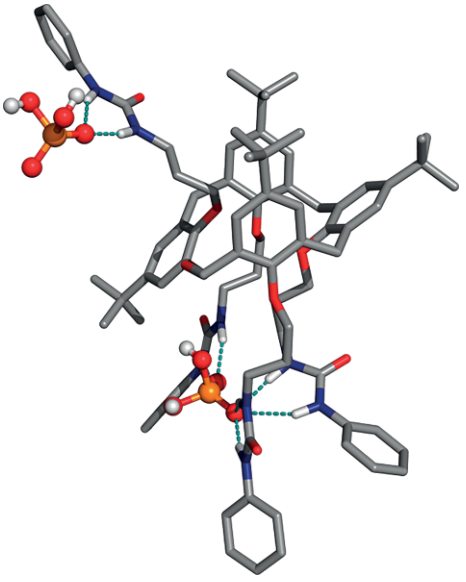

Figure 10. Illustrative snapshot of **4b**–$H_2PO_4^-$ (1:2) complex with the anions being recognised in the upper and lower rims by hydrogen bonds (light blue dashed lines). Remaining details as given in Figure 8.

Table 4. Average dimensions (distances and angles) and counting of hydrogen bonding interactions between **4b** and $H_2PO_4^-$ in 1:2 complex.

Position	Distance [Å]	Angle [°]	Total number hydrogen bonds[a]
Upper	2.851 ± 0.130[b]	158.3 ± 8.2[b]	2.14 ± 0.37
Lower	2.937 ± 0.231[c]	155.0 ± 11.9[c]	6.81 ± 0.96

[a] N = 8000. [b] N = 16000. [c] N = 48000.

Molecular Mechanics (MM) binding interaction energies were assessed for both binding arrangements in scenarios **A** and **B**, calculated as $\Delta E_{Total} = \Delta E_{ELEC} + \Delta E_{vdW} + \Delta E_{INT}$, where ΔE_{ELEC} and ΔE_{vdW} are the energy differences between the electrostatic and van der Waals components of the complex, **4b** and the anion. Moreover, the ΔE_{INT} component, related with the bond, angle and torsion angle terms, is zero given that all individual energy components of each partner were assessed from the MD simulations carried out for anion complexes. The average values of ΔE_{Total}, ΔE_{ELEC} and ΔE_{vdW} for the individual systems are given in Table S4, while the graphical comparison of ΔE_{Total} is shown in Figure 11. The anion recognition by hydrogen bonds is mainly dictated by electrostatic interactions and, consequently, the **A** binding arrangement is much more stable than the **B**, due to the higher number of phenylureido binding units involved in the anion recognition. For the majority of the anions studied, the ΔE_{Total} values follow the same trend of the binding affinity constants.

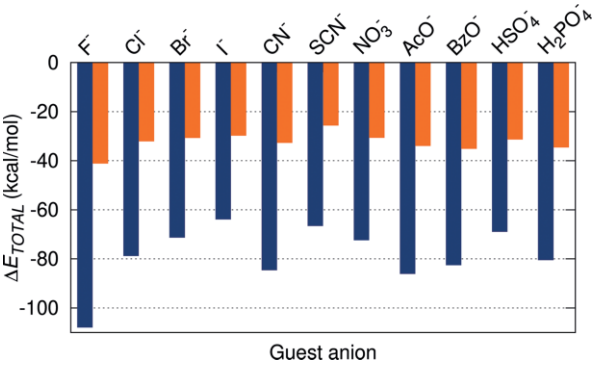

Figure 11. Comparison of the ΔE_{TOTAL} interaction energies assessed for the ion complexes of **4b** in binding arrangements **A** (blue) and **B** (orange).

Conclusions

Two new anion receptors based on dihomooxacalix[4]arenes bearing four urea units (*tert*-butyl **4a** and phenyl **4b**) at the lower rim linked by a propyl spacer were obtained in the partial cone-1 conformation in solution and in the solid state. The X-ray structures of both **4a** and **4b** were reported. Two crystal forms of **4a** were obtained from different solvents. All three centrosymmetric crystal structures confirmed the partial cone conformation of the dihomooxacalix[4]arenes and the presence of a racemic mixture of inherent chiral enantiomeric couples. A method has been proposed to assign the descriptors (M/P) of the absolute chirality. An extended H-bond network involving the ureido groups has been observed in the solid state. The host–guest properties of **4a** and **4b** were established by ^{1}H NMR, UV/Vis and MD studies. The formation of 1:1 complexes between anions of different geometries and receptors **4a** and **4b** (except in the case of $H_2PO_4^-$ and Ph urea **4b**) through hydrogen bonding was observed. *t*Bu urea **4a** was found to be a much weaker receptor than Ph urea **4b**, displaying association constants that in general decreased with decreasing of the anion basicity and showing the strongest complexation for F^-. The binding efficiency of Ph urea **4b** is clearly higher than those previously reported by other related dihomooxacalix[4]arene receptors. **4b** showed a remarkable affinity for Cl^- and mainly for BzO^- (log K_{ass} = 4.55 and 4.81, respectively), the latter value being the highest ever found with a dihomooxa receptor. Anions such as F^-, CN^-, AcO^- and HSO_4^- were also tightly bound by **4b**. Compared to the Ph urea analogue bearing a butyl spacer, it was found that the strong enhancement observed on **4b** binding ability is due to the shorter size of the spacer (propyl vs. butyl), and consequently to the less flexible and more pre-organized urea arms. Furthermore, it was demonstrated that anions are bound to the lower rim urea units, which provide a higher number of potential hydrogen-bond donor sites. This was corroborated by the structural and energetic findings obtained by the MD simulations.

These results suggest that dihomooxacalix[4]arenes bearing shorter spacers, and consequently less flexible urea arms, should present stronger anion complexation. Moreover, the use of such compounds as heteroditopic receptors will bring improvements, since ion pairs will be in a closer proximity. The

synthesis and study of ureido-homooxacalixarenes containing ethyl spacers are currently under investigation.

Experimental Section

Synthesis: All chemicals were reagent grade and were used without further purification. Chromatographic separations were performed on Merck silica gel 60 (particle size 40–63 μm, 230–400 mesh). Melting points were measured on a Stuart Scientific apparatus and are uncorrected. FTIR spectra were recorded on a Shimadzu Model IRaffinity-1 spectrophotometer. ^{1}H and ^{13}C NMR spectra were recorded on a Bruker Avance III 500 MHz spectrometer, with TMS as internal reference. The conventional COSY 45 and the phase-sensitive NOESY experiments were collected as 256 × 2 K complex points. ROESY spectra were acquired as 4096 × 256 complex points, with 128 scans per increment and a mixing time of 300 ms. Elemental analysis was determined on a Fisons EA 1108 microanalyser.

7,13,19,25-Tetra-*tert*-butyl-27,28,29,30-tetra[(3-phthalimidopropyl)oxy]-2,3-dihomo-3-oxacalix[4]arene (2): A mixture of *p-tert*-butyldihomooxacalix[4]arene (3 g, 4.42 mmol), *N*-(3-bromopropyl)phthalimide (7.25 g, 26.5 mmol), K_2CO_3 (3.67 g, 26.5 mmol) and KI (2.20 g, 13.3 mmol) in CH_3CN (130 mL) was refluxed and stirred under N_2 for 5 d. After cooling, the solvent was evaporated under reduced pressure and the residue was dissolved in CH_2Cl_2 (225 mL) and washed with 1 M HCl (2 × 150 mL), NH_4Cl saturated solution (2 × 150 mL) and brine (150 mL). The organic layer was dried with Na_2SO_4 and the solvents evaporated to dryness. The crude product was subjected to flash chromatography on silica gel (eluent gradient from *n*-hexane/ethyl acetate, 80:20 to 60:40) to afford a white solid in 39 % yield (2.45 g). An analytically pure sample was obtained from recrystallization from CH_2Cl_2/MeOH: m.p. 153–154 °C. IR (KBr): $\tilde{\nu}$ = 1713 (CO) cm^{-1}. ^{1}H NMR ($CDCl_3$, 500 MHz): δ = 0.94, 1.16 [2s, 36 H, $C(CH_3)_3$], 2.22–2.42 (several m, 8 H, $OCH_2CH_2CH_2N$), 3.19, 4.43 (ABq, J = 13.4 Hz, 4 H, $ArCH_2Ar$), 3.20, 4.38 (ABq, J = 12.9 Hz, 2 H, $ArCH_2Ar$), 3.72–3.82, 3.86–3.96 (4m, 16 H, $OCH_2CH_2CH_2N$), 4.63, 4.69 (ABq, J = 13.7 Hz, 4 H, CH_2OCH_2), 6.69, 6.94, 7.04 (3d, 8 H, ArH), 7.58 (m, 8 H, ArH-Pht), 7.67 (m, 8 H, ArH-Pht) ppm. ^{13}C NMR ($CDCl_3$, 125.8 MHz): δ = 29.56, 29.63 ($OCH_2CH_2CH_2NH_a$), 30.2, 30.7 ($ArCH_2Ar$), 31.4 (2C, $C(CH_3)_3$], 34.0 (2C, $C(CH_3)_3$], 35.6 (2C, $OCH_2CH_2CH_2NH_a$), 68.2 (CH_2OCH_2), 71.9, 72.4 ($OCH_2CH_2CH_2NH_a$), 123.0 (2C), 133.46, 133.49 (ArH-Pht), 123.5, 125.6 (2C), 125.8 (ArH), 131.2, 132.2, 132.3, 133.3 (2C), 134.0, 144.8, 145.2, 152.1, 152.8 (Ar), 168.17, 168.21 (CO) ppm. $C_{89}H_{94}N_4O_{13}$ (1427.74): calcd. C 74.87, H 6.64, N 3.92; found C 74.72, H 6.68, N 3.91.

7,13,19,25-Tetra-*tert*-butyl-27,28,29,30-tetra[(4-aminopropyl)oxy]-2,3-dihomo-3-oxacalix[4]arene (3): To a suspension of 1.20 g of **2** (0.84 mmol) in 50 mL of EtOH was added 8.15 mL (168 mmol) of hydrazine monohydrate. The mixture was refluxed and stirred under N_2 for about 14 h. After cooling, the solvent was evaporated under reduced pressure and the residue was dissolved in a CH_2Cl_2 (60 mL)/H_2O (60 mL) mixture and stirred for 30 min. The organic layer was dried with Na_2SO_4 and the solvent evaporated to give tetraamino **3** as a pale yellow solid (0.75 g, 98 % yield), which was pure enough to be immediately used in the next step. ^{1}H NMR ($CDCl_3$, 500 MHz): δ = 0.23, 0.38 (2m, 2 H, $OCH_2CH_2CH_2NH_2$ inverted), 1.22, 1.23, 1.28, 1.37 [4s, 36 H, $C(CH_3)_3$], 1.58, 1.67, 1.80–2.08 (several m, 16 H, $OCH_2CH_2CH_2NH_2$ and $OCH_2CH_2CH_2NH_2$ inverted) 2.18 (m, 2 H, $OCH_2CH_2CH_2NH_2$ inverted), 2.74–2.86 (m, 6 H, $OCH_2CH_2CH_2NH_2$), 3.27, 4.41 (ABq, J = 12.9 Hz, 2 H, $ArCH_2Ar$), 3.31, 4.42 (ABq, J = 12.8 Hz, 2 H, $ArCH_2Ar$), 3.50–3.65, 3.79 (2m, 6 H, $OCH_2CH_2CH_2NH_2$), 3.86 (s, 2 H, $ArCH_2Ar$ inverted), 4.03, 4.40 (ABq, J = 11.6 Hz, 2 H, CH_2OCH_2), 4.10, 4.85 (ABq, J = 11.0 Hz, 4 H, CH_2OCH_2), 7.04, 7.06, 7.11, 7.17, 7.20, 7.23, 7.24, 7.28 (8d, 8 H, ArH) ppm.

Procedure for the Synthesis of Ureas 4a and 4b: To a solution of **3** (0.75 g, 0.83 mmol) in $CHCl_3$ (35 mL) was added 3.31 mmol of the appropriate isocyanate. The mixture was stirred at room temperature under N_2 for 4 h. Evaporation of the solvent yielded the crude products which were purified as described below.

7,13,19,25-Tetra-*tert*-butyl-27,28,29,30-tetra{[(*N*′-*tert*-butylureido)propyl]oxy}-2,3-dihomo-3-oxacalix[4]arene (4a): Flash chromatography (SiO_2, eluent CH_2Cl_2/MeOH, from 99:1 to 97:3); it was obtained in 61 % yield (0.66 g); m.p. 208–210 °C. IR (KBr): $\tilde{\nu}$ = 3374 (NH), 1641 (C=O) cm^{-1}. ^{1}H NMR ($CDCl_3$, 500 MHz): δ = 0.03, 0.13 (2m, 2 H, $OCH_2CH_2CH_2NH_a$ inverted), 1.14, 1.26, 1.28, 1.35 [4s, 36 H, $C(CH_3)_3$], 1.25, 1.31, 1.34, 1.35 [4s, 36 H, $NH_bC(CH_3)_3$], 1.58, 1.81 (2m, 6 H, $OCH_2CH_2CH_2NH_a$), 2.05, 2.59 (2m, 2 H, $OCH_2CH_2CH_2NH_a$ inverted), 2.27, 2.52 (2m, 2 H, $OCH_2CH_2CH_2NH_a$ inverted), 3.11, 3.17–3.35 (several m, 6 H, $OCH_2CH_2CH_2NH_a$), 3.27, 4.33 (ABq, J = 12.9 Hz, 2 H, $ArCH_2Ar$), 3.28, 4.36 (ABq, J = 12.7 Hz, 2 H, $ArCH_2Ar$), 3.58, 3.66, 3.77 (3m, 6 H, $OCH_2CH_2CH_2NH_a$), 3.87 (m, 2 H, $ArCH_2Ar$ inverted), 4.03 (s, 1 H, NHb inverted), 4.08, 4.45 (ABq, J = 11.7 Hz, 2 H, CH_2OCH_2), 4.12, 4.81 (ABq, J = 10.9 Hz, 2 H, CH_2OCH_2), 4.45 (t, 1 H, NHa inverted), 5.06, 5.21, 5.38 (3s, 3 H, NHb), 5.28, 5.38, 5.66 (3t, 3 H, NHa), 6.96, 7.03, 7.06, 7.11, 7.22, 7.28, 7.30 (7d, 8 H, ArH) ppm. ^{13}C NMR ($CDCl_3$, 125.8 MHz): δ = 28.2, 29.2, 30.0, 30.4, 30.8 ($OCH_2CH_2CH_2NH_a$ and $ArCH_2Ar$), 29.62, 29.64, 29.68, 29.71 [$NH_bC(CH_3)_3$], 31.37, 31.49, 31.53, 31.7 [$C(CH_3)_3$], 34.07, 34.11, 34.18, 34.21 [$C(CH_3)_3$], 36.6, 37.10, 37.16, 37.8, 39.3 ($ArCH_2Ar$ and $OCH_2CH_2CH_2NH_a$), 49.9, 50.0, 50.1, 50.2 [$NH_bC(CH_3)_3$], 65.8, 66.2 (CH_2OCH_2), 71.0, 72.1, 72.7, 72.8 ($OCH_2CH_2CH_2NH_a$), 125.2, 125.4, 125.6, 126.3, 126.6, 126.8, 128.1, 128.3 (ArH), 129.5, 129.7, 132.6, 132.8, 133.0, 134.0, 134.6, 135.1, 145.2, 145.5, 145.9, 146.2, 152.4, 153.3, 153.8, 154.9 (Ar), 157.5, 158.4 (2C), 158.5 (CO) ppm. $C_{77}H_{122}N_8O_9$ (1303.86): calcd. C 70.93, H 9.43, N 8.59; found C 71.07, H 9.44, N 8.32.

7,13,19,25-Tetra-*tert*-butyl-27,28,29,30-tetra{[(*N*′-phenylureido)propyl]oxy}-2,3-dihomo-3-oxacalix[4]arene (4b): Flash chromatography (SiO_2, eluent CH_2Cl_2/MeOH, 99:1) followed by recrystallization from CH_2Cl_2/*n*-hexane; it was obtained in 46 % yield (0.49 g); m.p. 231–231 °C. IR (KBr): $\tilde{\nu}$ = 3337 (NH), 1647 (CO) cm^{-1}. ^{1}H NMR ($CDCl_3$, 500 MHz): δ = –0.25, 0.07 (2m, 2 H, $OCH_2CH_2CH_2NH_a$ inverted), 1.20, 1.22, 1.23, 1.24 [4s, 36 H, $C(CH_3)_3$], 1.66–1.90 (several m, 6 H, $OCH_2CH_2CH_2NH_a$), 2.12, 2.30 (2m, 2 H, $OCH_2CH_2CH_2NH_a$ inverted), 2.62 (m, 2 H, $OCH_2CH_2CH_2NH_a$ inverted), 3.17–3.34, 3.40, 3.52, 3.61–3.75, 3.87 (several m, 12 H, $OCH_2CH_2CH_2NH_a$), 3.30, 4.33 (ABq, J = 12.8 Hz, 2 H, $ArCH_2Ar$), 3.31, 4.36 (ABq, J = 12.8 Hz, 2 H, $ArCH_2Ar$), 3.54, 3.79 (ABq, J = 16.8 Hz, 2 H, $ArCH_2Ar$ inverted), 4.16, 5.00 (ABq, J = 11.3 Hz, 2 H, CH_2OCH_2), 4.19, 4.43 (ABq, J = 11.4 Hz, 2 H, CH_2OCH_2), 5.19, 5.53, 5.87, 6.01 (4t, 4 H, NH_a), 6.09 (s, 1 H, NH_b inverted), 6.83, 7.08, 7.10, 7.12, 7.18, 7.19, 7.30, 7.33 (8d, 8 H, ArH), 6.89–7.21 (several m, 4 H, Ph-H_p), 7.05–7.25, 7.35, 7.39 (several m, 16 H, Ph-H_m and Ph-H_o), 7.47, 7.64, 7.79 (3s, 3 H, NH_b) ppm. ^{13}C NMR ($CDCl_3$, 125.8 MHz): δ = 27.9, 28.8, 29.7, 30.4, 30.5, 30.9 ($OCH_2CH_2CH_2NH_a$ and $ArCH_2Ar$), 31.38 (2C), 31.44, 31.5 [$C(CH_3)_3$], 34.1 (2C), 34.17, 34.20 [$C(CH_3)_3$], 36.9, 37.0, 37.6, 38.4, 39.1 ($ArCH_2Ar$ and $OCH_2CH_2CH_2NH_a$), 66.4, 68.3 (CH_2OCH_2), 71.2, 72.3, 72.5, 72.7 ($OCH_2CH_2CH_2NH_a$), 119.4, 119.6, 119.8, 121.2, 125.72, 125.75, 126.51, 126.53, 128.9, 129.04, 129.06, 129.11 (Ph-ArH), 122.5, 122.6, 123.0, 123.5, 126.0, 126.9, 128, 3, 128.8 (ArH), 129.2, 132.4, 132.9, 133.5, 133.6, 134.2, 134.7, 138.7, 139.0, 139.2, 139.4, 145.8, 146.0, 146.1, 146.3, 152.3, 153.0, 154.0 (Ar), 155.2, 156.5, 156.6, 156.8 (CO) ppm. $C_{85}H_{106}N_8O_9$ (1383.82): calcd. C 73.78, H 7.72, N 8.10; found C 73.77, H 7.71, N 8.14.

Determination of the Crystallographic Structures of Compounds 4a and 4b:

CCDC 1813152 (for **4aα**), 1839628 (for **4aβ**), and 1590174 (for **4b**) contain the supplementary crystallographic data for this paper. These data can be obtained free of charge from The Cambridge Crystallographic Data Centre.

^{1}H NMR Titrations: The association constants (as log K_{ass}) were determined in $CDCl_3$ by ^{1}H NMR titration experiments. Several aliquots (up to 10 equiv.) of the anion solutions (as TBA salts) were added to 0.5 mL solution of the receptors (2.5×10^{-3}–5×10^{-3} M for *t*Bu–urea and 8.3×10^{-4} M for Ph-urea due to its lower solubility in chloroform) directly in the NMR tube. The spectra were recorded after each addition of the salts, and the temperature of the NMR probe was kept constant at 25 °C. For each anion-receptor system titrations were repeated at least two times. The association constants were evaluated using the WinEQ NMR 2 program[29] and following the urea NH chemical shifts. The Job methods were performed keeping the total concentration in the same range as before.

UV/Vis Titrations: The association constants were also determined in $CHCl_3$ by absorption spectrophotometry at 25 °C. The spectra were recorded between 250 and 300 nm, using quartz cells with an optical path length of 1 cm. Several aliquots (up to 10 equiv.) of the anion solutions (as TBA salts) were directly added into the cell containing 2 mL of the receptor solution (5×10^{-5} M). The spectral changes were interpreted using the HypSpec 2014 program.[36]

Acknowledgments

This work was supported by CQE, Project ref. UID/QUI/00100/2013 and by CICECO - Aveiro Institute of Materials, Project ref. UID/CTM/50011/2013, financed by National Funds through the FCT/MEC and co-financed by QREN-FEDER through COMPETE under the PT2020 Partnership Agreement. The University of Trieste is acknowledged for financial support, FRA2016.

Keywords: Dihomooxacalix[4]arenes · Tetraureido anion receptors · X-ray diffraction · NMR studies · MD simulations

[1] N. H. Evans, P. D. Beer, *Angew. Chem. Int. Ed.* **2014**, *53*, 11716–11754; *Angew. Chem.* **2014**, *126*, 11908.
[2] N. Busschaert, C. Caltagirone, W. Van Rossom, P. A. Gale, *Chem. Rev.* **2015**, *115*, 8038–8155.
[3] G. Ramezani, N. Valaie, V. Rakhshan, *Dent. Res. J.* **2015**, *12*, 31–37.
[4] C. D. Gutsche, *Calixarenes, An Introduction*; Monographs in Supramolecular Chemistry; The Royal Society of Chemistry, Cambridge, **2008**.
[5] *Calixarenes and Beyond* (Eds.: P. Neri, J. L. Sessler, M-X. Wang); Springer International Publishing Switzerland, **2016**.
[6] S. E. Matthews, P. D. Beer, *Supramol. Chem.* **2005**, *17*, 411–435.
[7] R. Joseph, C. P. Rao, *Chem. Rev.* **2011**, *111*, 4658–4702.
[8] N. Y. Edwards, A. L. Possanza, *Supramol. Chem.* **2013**, *25*, 446–463.
[9] J. Scheerder, M. Fochi, F. J. Engbersen, D. N. Reinhoudt, *J. Org. Chem.* **1994**, *59*, 7815–7820.
[10] E. Quinlan, S. E. Matthews, T. Gunnlaugsson, *J. Org. Chem.* **2007**, *72*, 7497–7503.
[11] I. Stibor, J. Budka, V. Michlova, M. Tkadlecova, M. Pojarova, P. Curinova, P. Lhotak, *New J. Chem.* **2008**, *32*, 1597–1607.
[12] P. Curinova, I. Stibor, J. Budka, J. Sykora, L. Kamil, P. Lhotak, *New J. Chem.* **2009**, *33*, 612–619.
[13] J. N. Babu, V. Bhalla, M. Kumar, R. K. Puri, *New J. Chem.* **2009**, *33*, 675–681.
[14] T. Klejch, J. Slavicek, O. Hudecek, V. Eigner, N. A. Gutierrez, P. Curinova, P. Lhotak, *New J. Chem.* **2016**, *40*, 7935–7942.
[15] M. Rezankova, J. Budka, J. Miksatko, V. Eigner, I. Cisarova, P. Curinova, P. Lhotak, *Tetrahedron* **2017**, *73*, 742–749.
[16] C. Capici, R. De Zorzi, C. Gargiulli, G. Gattuso, S. Geremia, A. Notti, S. Pappalardo, M. F. Parisi, F. Puntoriero, *Tetrahedron* **2010**, *66*, 4987–4993.
[17] J. Scheerder, F. J. Engbersen, A. Casnati, R. Ungaro, D. N. Reinhoudt, *J. Org. Chem.* **1995**, *60*, 6448–6454.
[18] M. Hamon, M. Ménand, S. Le Gac, M. Luhmer, V. Dalla, I. Jabin, *J. Org. Chem.* **2008**, *73*, 7067–7071.
[19] A. Nehra, S. Bandaru, D. S. Yarramala, C. P. Rao, *Chem. Eur. J.* **2016**, *22*, 8903–8914.
[20] S. Rahman, H. Tomiyasu, H. Kawazoe, J. L. Zhao, H. Cong, X. L. Ni, X. Zeng, M. R. J. Elsegood, T. G. Warwick, S. J. Teat, C. Redshaw, P. E. Georghiou, T. Yamato, *New J. Chem.* **2016**, *40*, 9245–9251.
[21] P. M. Marcos, F. A. Teixeira, M. A. P. Segurado, J. R. Ascenso, R. J. Bernardino, S. Michel, V. Hubscher-Bruder, *J. Org. Chem.* **2014**, *79*, 742–751.
[22] P. M. Marcos, F. A. Teixeira, M. A. P. Segurado, J. R. Ascenso, R. J. Bernardino, G. Brancatelli, S. Geremia, *Tetrahedron* **2014**, *70*, 6497–6505.
[23] F. A. Teixeira, P. M. Marcos, J. R. Ascenso, G. Brancatelli, N. Hickey, S. Geremia, *J. Org. Chem.* **2017**, *82*, 11383–11390.
[24] P. M. Marcos, *Calixarenes and Beyond* (Eds.: P. Neri, J. L. Sessler, M-X. Wang); Springer International Publishing Switzerland, **2016**, pp. 445–466.
[25] a) Conformation *partial cone 1* was previously named *partial cone A*; b) P. M. Marcos, J. R. Ascenso, R. Lamartine, J. L. C. Pereira, *Tetrahedron* **1997**, *53*, 11791–11802.
[26] C. Jaime, J. de Mendoza, P. Prados, P. Nieto, C. Sanchez, *J. Org. Chem.* **1991**, *56*, 3372–3376.
[27] P. M. Marcos, J. R. Ascenso, R. Lamartine, J. L. C. Pereira, *J. Org. Chem.* **1998**, *63*, 69–74.
[28] A. Szumna, *Chem. Soc. Rev.* **2010**, *39*, 4274–4285.
[29] M. J. Hynes, *J. Chem. Soc., Dalton Trans.* **1993**, 311–312.
[30] D. A. Case, D. S. Cerutti, T. E. Cheatham, III, T. A. Darden, R. E. Duke, T. J. Giese, H. Gohlke, A. W. Goetz, D. Greene, N. Homeyer, S. Izadi, A. Kovalenko, T. S. Lee, S. LeGrand, P. Li, C. Lin, J. Liu, T. Luchko, R. Luo, D. Mermelstein, K. M. Merz, G. Monard, H. Nguyen, I. Omelyan, A. Onufriev, F. Pan, R. Qi, D. R. Roe, A. Roitberg, C. Sagui, C. L. Simmerling, W. M. Botello-Smith, J. Swails, R. C. Walker, J. Wang, R. M. Wolf, X. Wu, L. Xiao, D. M. York, P. A. Kollman, *AMBER 2016*; University of California: San Francisco, **2016**.
[31] J. Wang, R. M. Wolf, J. W. Caldwell, P. A. Kollman, D. A. Case, *J. Comput. Chem.* **2004**, *25*, 1157–1174.
[32] J. Wang, R. M. Wolf, J. W. Caldwell, P. A. Kollman, D. A. Case, *J. Comput. Chem.* **2005**, *26*, 114–114.
[33] C. I. Bayly, P. Cieplak, W. D. Cornell, P. A. Kollman, *J. Phys. Chem.* **1993**, *97*, 10269–10280.
[34] P. Li, L. F. Song, K. M. Merz Jr., *J. Chem. Theory Comput.* **2015**, *11*, 1645–1657.
[35] T. Fox, P. A. Kollman, *J. Phys. Chem. B* **1998**, *102*, 8070–8079.
[36] P. Gans, A. Sabatini, A. Vacca, *Talanta* **1996**, *43*, 1739–1753.